

PAPER • OPEN ACCESS

CFD prediction of air flow characteristics along the profile of a rural house model located on different ridge terrain height

To cite this article: J Abdullah *et al* 2019 *IOP Conf. Ser.: Earth Environ. Sci.* **244** 012008

View the [article online](#) for updates and enhancements.

You may also like

- [Investigations into the Interaction of a Wind Turbine with Atmospheric Turbulence in Complex Terrain](#)
C Schulz, L Klein, P Weihing *et al.*
- [Wind tunnel testing of a wind turbine in complex terrain](#)
Emmanouil M Nanos, Kutay Yilmazlar, Alex Zanotti *et al.*
- [A Local Update and Refinement method of the Global Terrain Nature Grid](#)
Hongbin Wang, Junwu Zhao, Yuanlin Liu *et al.*



ECS
The
Electrochemical
Society
Advancing solid state &
electrochemical science & technology

DISCOVER
how sustainability
intersects with
electrochemistry & solid
state science research

CFD prediction of air flow characteristics along the profile of a rural house model located on different ridge terrain height

J Abdullah¹, S S Zaini¹, M S Abdul Aziz², T A Majid¹, W N W Yahya¹ and S N C Deraman¹

¹Disaster Research Nexus, School of Civil Engineering, Engineering Campus, Universiti Sains Malaysia

²School of Mechanical Engineering, Engineering Campus, Universiti Sains Malaysia

Email: ceshaharudin@usm.my

Abstract. Rural houses are classified as low rise and non-engineered building. These types of structures are at risk of getting damage during a windstorm event. Many studies have been conducted to investigate the air flow characteristic using CFD for structures located on flat terrain. However, wind that passes a ridge terrain has stronger wind speed and can be a potential hazard to rural houses located on top of it. This study investigates the air flow characteristics along the 2-D profile of a rural house model located on top of a ridge terrain considering the effect of varying the terrain height. Computational Fluid Dynamics method was used with the aid of ANSYS FLUENT software package. The results presented in this study are in term of pressure coefficient both with positive and negative values. The flow patterns over the models are observed using streamline. The result showed the ridge terrain height influenced the pressure coefficient and flow pattern. The highest suction was observed for the steepest ridge terrain due to the build-up in the local up-slope wind acceleration.

1. Introduction

Usually, the failure of roof occurs during the event of high wind speed. Bachok et al. [1] stated that strong winds with high speeds can cause significant damage to a structure. The damage can be severe for the case of non-engineered rural houses. The damages can be severe if the wind speed can be escalated in the case of wind passing over a ridge terrain. Several codes [2-3] incorporate hill shape and terrain multiplier to estimate the design wind speed as well as the anticipated pressure coefficients surrounding the house. Similarly, a number of studies have been conducted to investigate the air flow characteristics surrounding a low-rise building model using Computational Fluid Dynamics (CFD) simulations [4-6]. However, the studies mainly consider flat terrain condition. Nevertheless, many simulations have been conducted to investigate the change in the pressure contour and streamlines pattern due to the variation of terrain types. The CFD simulations were performed in 2-D surrounding [7-9] but not considering the pressure distribution along a house model. This study aims to determine the sensitivity of ridge terrain height with respect to the distribution of pressure coefficient along a rural house model using CFD method in 2-D environment.

2. Methodology

This section briefly discusses the numerical procedures of the CFD method. The model of the rural house was generated using ANSYS Design Modeller and the analysis was performed with the aid of ANSYS Fluent 14 commercial software.



2.1. Building Data

The title Figure 1 shows the cross section and relevant dimensions of the rural model. Typically in Malaysia, a rural house carries the feature of having a core house with an extension (commonly known as kitchen house). This model represents the average dimensions of the rural house located in the northern region of Peninsula Malaysia as reported by Zaini et al. [10]. In this model, the gap height between the core and the extension house and the roof pitch were set to be 1.1 m and 22° , respectively. For ease of discussion, the section of the house model was divided into nine regions namely:

- Zone A (windward wall of kitchen house)
- Zone B (windward roof overhang of kitchen house)
- Zone C (windward roof of kitchen house)
- Zone D (windward wall of core house)
- Zone E (windward roof overhang of core house)
- Zone F (windward roof of core house)
- Zone G (leeward roof of core house)
- Zone H (leeward roof overhang of core house)
- Zone I (leeward wall of core house)

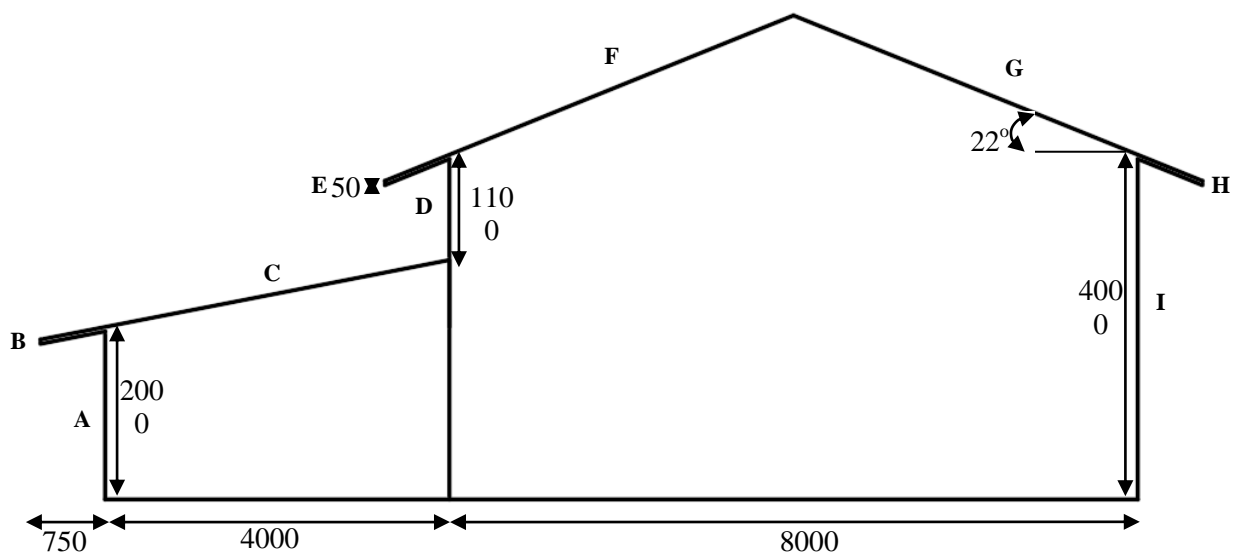
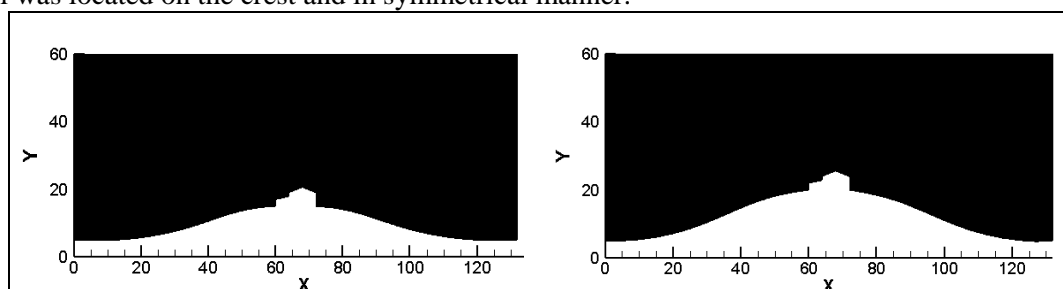


Figure 1. Sectional view and basic dimension of the rural house model (all dimensions in mm)

2.2. Topography Characteristics

This study only considers the ridge type terrains with varying height as shown in Figure 2. The slope of the ridge was calculated as the angle bounded by the flat ground at the inlet up to the crest. For this study, terrain slope angles of approximately 14° , 18° , 23° and 27° were considered. The rural house model was located on the crest and in symmetrical manner.



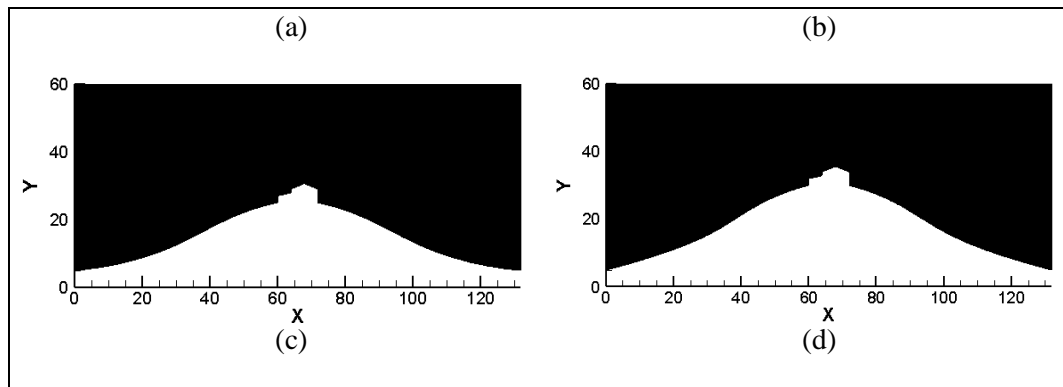


Figure 2. Topography characteristic for terrain model (a) Ridge 14° (b) Ridge 18° (c) Ridge 23° and (d) Ridge 27°

2.3. Computational Domain

The lateral distance of $15H$, measured from the inlet and outlet to the end of the uprising slope was set as the lateral domain. The minimum clearance height of $5H$ was used for the top boundary condition. H denotes the height of the building model and the rural house model adopted $H = 4$ m [10]. The computational domain follows the recommendation stated by Shirasawa et al. [11] and Mochida et al. [12] that specified the lateral and top boundary should be set at $5H$ or more, away from the building while the outflow boundary should be at least $15H$ behind the building [13]. These dimensions were used in order to avoid obstruction to the flow development. The blockage ratio was calculated to be in the range of $0.85 - 0.95\%$ (less than 3%) following the recommendation from Tominaga et al. [14]. Finally, the roughness height (K_s) and roughness constant (C_s) was fixed at 0.035 m and 1.0 , respectively. Figure 3 shows the overall boundary condition of the computational domain for the model with ridge terrain characteristic.

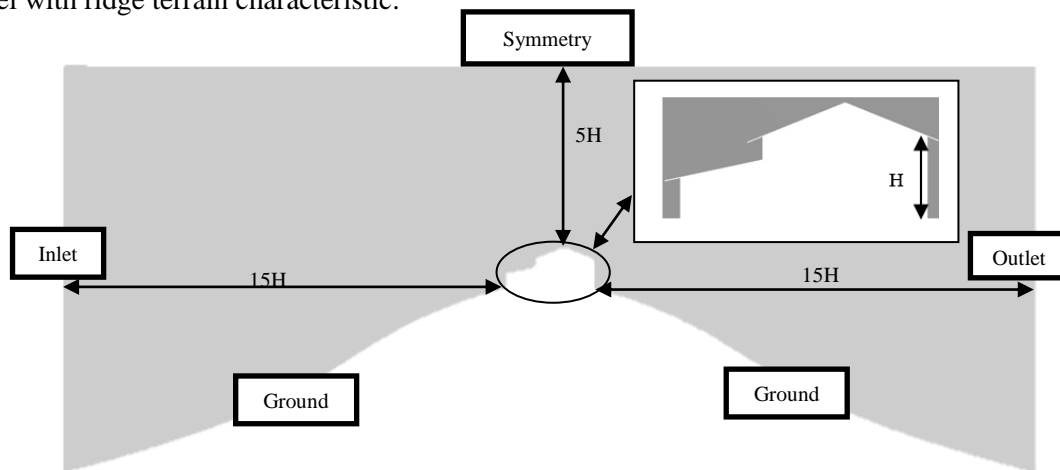


Figure 3. Boundary condition of the computational domain for a model with ridge terrain

2.4. Model Generation

The maximum and minimum face sizes were controlled in order to generate the adequate number of mesh. The final mesh computed for the Ridge 14° , Ridge 18° , Ridge 23° and Ridge 27° were 304 398, 287 995, 267 343 and 255 265, respectively. RNG $k-\epsilon$ model was used in this study due to the fact that it is able to exhibit good performance in predicting of the turbulent kinetic energy [4].

The mean velocity was obtained using:

$$v_x = v_{x,free} \left(\frac{y}{\delta}\right)^\alpha \quad (1)$$

The turbulence kinetic energy was calculated as follow:

$$k = \frac{u^*}{\sqrt{c_\mu}} \quad (2)$$

$$u^* = \frac{\kappa v}{\ln\left[\frac{H+z_0}{z_0}\right]} \quad (3)$$

The dissipation rate is:

$$\varepsilon = \frac{u^{*2}}{k(z+z_0)} \quad (4)$$

Where,

κ	=	Von Karman constant (0.4)
v_x	=	mean velocity
z_0	=	roughness length (0.035)
H	=	height of building (4 m)
c_μ	=	0.085

3. Result and Discussion

This section presents the simulation results and the discussions accordingly

3.1. Pressure Coefficient

The pressure of house was calculated using Tominaga et al [2],

$$C_p = P_s - P_{ref} / 0.5\rho U_{He}^2 \quad (5)$$

Where:

C_p	=	pressure coefficient
P_s	=	static pressure at the wall surfaces
P_{ref}	=	reference pressure
ρ	=	air density
U_{He}	=	velocity

Figure 4 shows the distribution of the pressure coefficient along the profile of the house models. It can be seen that the distribution pattern is almost similar. Unlike the case of a flat terrain, the coefficients were mainly in negative values (suction). In Zone A, the coefficients showed the minimum values suggesting the initiation of the suction. There was a sudden drop in Zone B where the suction started to build up due to the presence of the first overhang roof at the kitchen house. Following that, the suction started to decrease as the wind flow over the roof of the kitchen house. The suction showed a sharp drop as the wind flow from the overhang roof of the core house towards the roof ridge. All models exhibited maximum suction at the ridge. The suction decreased as the wind entered the leeward side and became stable along the leeward wall of the core house. The maximum pressure coefficients recorded at this point for Ridge 14⁰, Ridge 18⁰, Ridge 23⁰ and Ridge 27⁰ were -6.13, -9.53, -12.59 and -18.92, respectively. The model located on the steepest slope exhibited the highest negative coefficient due to the buildup of the local up-slope wind acceleration.

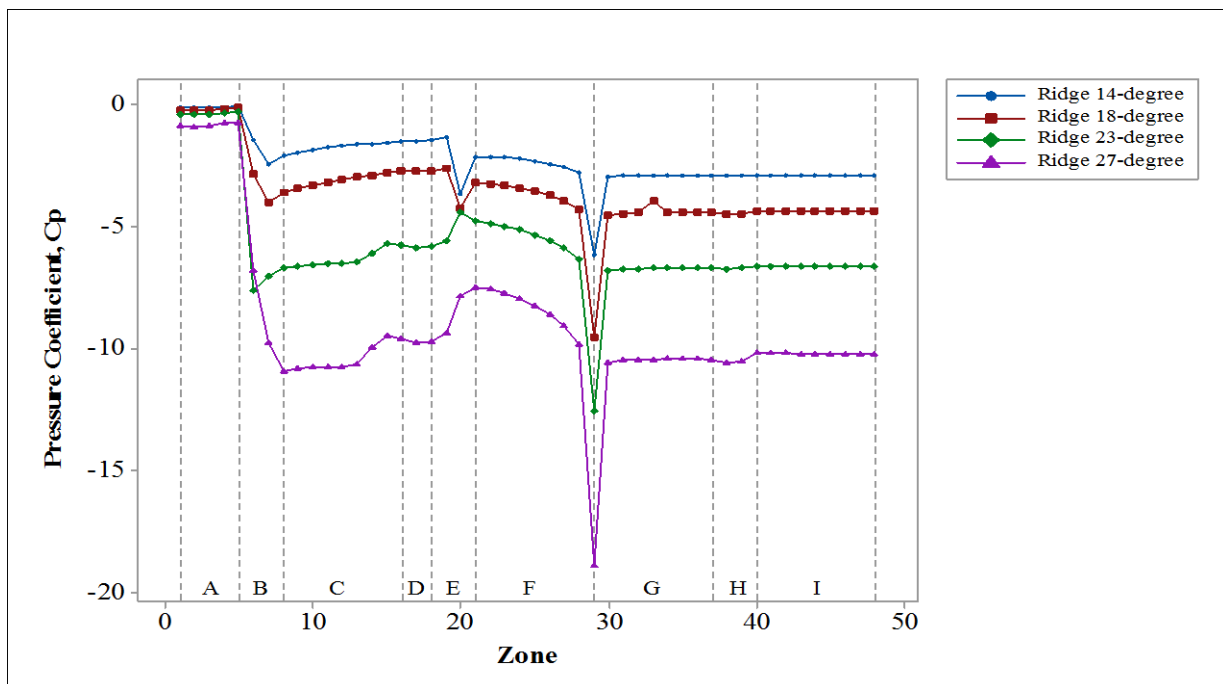


Figure 4. Pressure coefficient distribution of house for Ridge terrain model

Figure 5 shows the maximum negative pressure coefficient (suction) for all models. In general, the highest suction was recorded by model Ridge 27-Degree (-18.92) followed by Ridge 23-Degree (-12.59), Ridge 18-Degree (-9.53) and Ridge 14-Degree (-6.13). The chart shows that the relationship between the slope of the ridge terrain and the magnitude of the suction is not linear. The findings revealed that when the slope increased twofold, the magnitude of the maximum suction increased almost threefold.

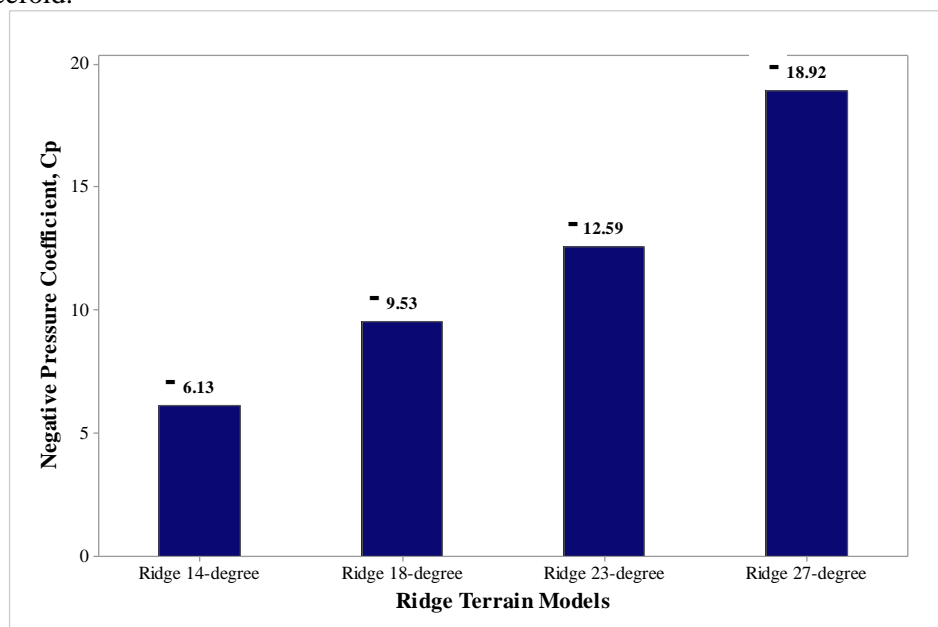


Figure 5. Summary for Ridge Terrain Models

Figure 6 shows the contour profile of the of pressure coefficient for ridge topography terrain. In can be seen that in all cases, the intensity of the suction effect become significant as the wind flow along the local upslope. As the slope of the ridge becomes steeper, the air flow regime manifested via the pressure coefficient contour exhibits drastic changes throughout the profile. The impact of magnifying

the magnitude of the suction was also extended along the roof of the house model as discussed earlier in section 3.1.

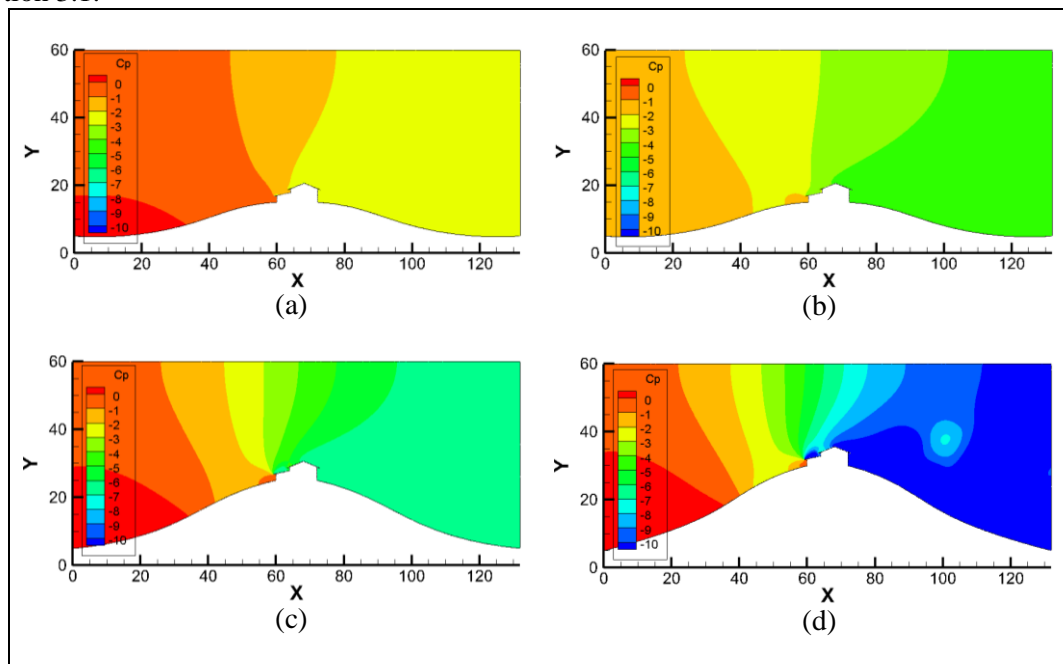


Figure 6. Pressure coefficient contour Ridge Terrain Model with slope angle (a) 14° (b) 18° (c) 23° and (d) 27°

3.2. Streamlines

Streamlines represent the direction and pattern of the wind flow. Figure 7 shows the flow pattern for different ridge terrain characteristics. Generally, the same streamlines pattern was observed in front of the house for all models. Formation of small eddy was observed at the extension house. This phenomenon is due to the fact that the up-slope wind was blocked by the wall of the kitchen house and produced reverse flow. At the leeward region of the house, the recirculation region was enlarged and increased the suction effect.

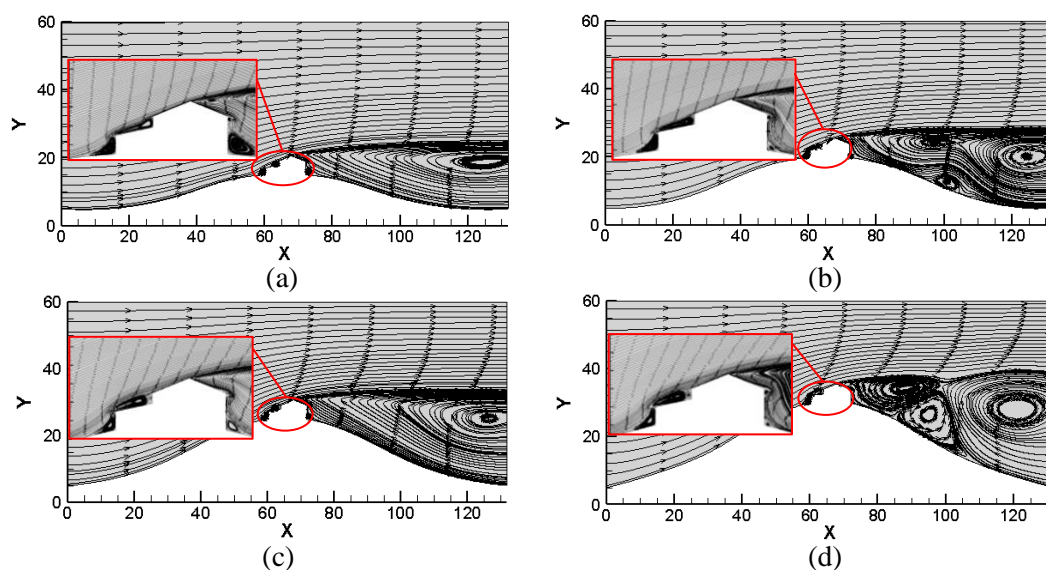


Fig. 7. Streamline pattern for Ridge Terrain Model with slope angle (a) 14° (b) 18° (c) 23° and (d) 27°

4. Conclusion

The research was carried out to investigate the distribution of pressure coefficient along the surface of the wall and the roof of rural house situated on a ridge terrain. The variable was the difference in the terrain height. The findings concluded that a ridge terrain with steeper slope developed high suction effect due to the built up of the local up-slope wind acceleration. The relationship between the slope angle and the pressure coefficient was found to be non-linear and can significantly increase the magnitude of the suction. As such, the incorporation of terrain types in CFD analysis is important in order to have a better understanding on the air flow characteristic surrounding a structure.

5. References

- [1] Bachok M F, Shamsudin S, Abidin R 2015 *International Journal of Environmental Science and Development* vol. 6, pp 625-642
- [2] Department of Standard Malaysia 2002 *Malaysian Standard:Code of Practice on Wind Loading for Building Structure*
- [3] Standards Australia Internatinal Ltd and Standards New Zealand 2011 *Australia/New Zealand Standard:Structural Design Action. Part 2: Wind Actions.*
- [4] Tominaga Y, Akabayashi S, Kitahara T, and Arinami Y 2015 *Journal of Building and Enviroment* vol 84, pp 204-213
- [5] Charisi S, Waszczuk M, and Thiis T K 2017 *Int. Conf. on Future building & Districts (Switzerland)* vol 122 (Elsevier) pp 637-642
- [6] Kuroyanagi T 2017 *Journal of Biosystem Engineering* vol 163, pp 15-27.
- [7] Feng W, Komle N I, Niu Y, Sun Z, Li G, and Yu W 2011 *Journal of Cold Region and Technology* vol 68, pp 162-172
- [8] Bitsuamulak G T, Stathopoulos T, ASCE F, and Bedard C 2004 *Journal of Aerospace Engineering* vol 21, Pp 384-392
- [9] Bitsuamulak G T, Bedard C, ASCE F and Stathopoulos T, 2007 *Journal of Computing in Civil Engineering* vol 12, pp 135-145
- [10] Zaini SS, Majid T A, Deraman S N C, Chik F A W, and Muhammad M K A 2017 *Int. Simposium on Civil and Enviromental Engineering (Malaysia)* vol 103 (EDP Sciences)
- [11] Shirasawa T, Tominaga Y, Yoshie R, Mochida A, Yoshino H, Kataoka H and Nozu T 2003 *Journal Technol. Des* vol 18, pp 169-174
- [12] Mochida A, Tominaga Y, Murakami S, Yoshie R, Ishihara T, and Ooka R 2002 *Wind Struct* vol 5 (2-4) pp 227-244
- [13] Franke J, Hellsten A, Schlunzen H, and Carissimo B 2007 *Title of the Book and Action Number*, pp 17-18
- [14] Tominaga Y, Mochida A, Yoshie R, Kataoka H, Nozu T, Yoshikawa M and Shirasawa T 2008 *Journal of Wind Engineering and Industrial Aerodynamics* vol 96, pp 1749-1761

Acknowledgments

The authors express their gratitude for the financial support of the Fundamental Research Grant Scheme (FRGS) from the Ministry of Higher Education Grant (203.PAWAM.6071317) and Universiti Sains Malaysia for providing the facilities.